

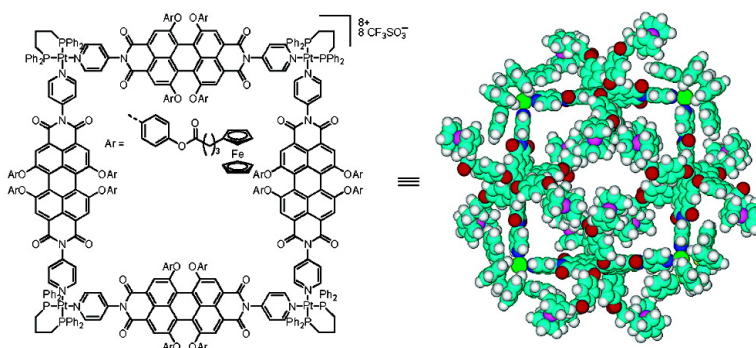
Article

# Self-Assembly of Ferrocene-Functionalized Perylene Bisimide Bridging Ligands with Pt(II) Corner to Electrochemically Active Molecular Squares

Chang-Cheng You, and Frank Wrthner

*J. Am. Chem. Soc.*, **2003**, 125 (32), 9716-9725 • DOI: 10.1021/ja029648x • Publication Date (Web): 11 July 2003

Downloaded from <http://pubs.acs.org> on March 29, 2009



## More About This Article

Additional resources and features associated with this article are available within the HTML version:

- Supporting Information
- Links to the 19 articles that cite this article, as of the time of this article download
- Access to high resolution figures
- Links to articles and content related to this article
- Copyright permission to reproduce figures and/or text from this article

[View the Full Text HTML](#)



**ACS Publications**  
 High quality. High impact.

# Self-Assembly of Ferrocene-Functionalized Perylene Bisimide Bridging Ligands with Pt(II) Corner to Electrochemically Active Molecular Squares

Chang-Cheng You and Frank Würthner\*

Contribution from the Institut für Organische Chemie, Universität Würzburg, Am Hubland, 97074 Würzburg, Germany

Received December 9, 2002; Revised Manuscript Received May 30, 2003; E-mail: wuerthner@chemie.uni-wuerzburg.de

**Abstract:** Ferrocenyl-substituted *N,N'*-di(4-pyridyl)perylene bisimide ligands have been synthesized by the coupling reaction of hydroxyphenoxy-perylene bisimides with ferrocenyl carboxylic acids. By means of metallosupramolecular self-assembly, hitherto unprecedented multiredox active dendritic molecular squares with 16 ferrocene groups positioned in the bridging ligands are prepared from the perylene bispyridyl imide ligands and [Pt(dppp)](OTf)<sub>2</sub> (dppp = 1,3-bis(diphenylphosphano)propane; OTf = trifluoromethanesulfonate) corner in high yield. The isolated metallosupramolecular squares were characterized by elemental analysis, <sup>1</sup>H, <sup>31</sup>P{<sup>1</sup>H} NMR, and UV/vis spectroscopy. The electrochemical properties of the ligands and squares are investigated by cyclic voltammetry as well as spectroelectrochemistry. The results obtained show that the redox behavior of ferrocene units is influenced by the square superstructure. Furthermore, redox titration of free ligand and corresponding molecular square with the one-electron oxidant thianthrenium pentachloroantimonate reveals that ferrocene groups in these structures may be oxidized completely by this oxidant, and highly charged species generated through oxidation of ferrocenyl groups in molecular square cause decomposition of the assembly due to pronounced Coulombic repulsion.

## Introduction

The self-assembly approach based on noncovalent coordinative bonding offers an attractive alternative to the conventional organic route for the preparation of structurally demanding functional systems. Thus, in the past decade much attention has been paid to the transition metal-mediated self-assembling process to provide diverse functional supramolecular architectures,<sup>1</sup> including linear polymers,<sup>2</sup> planar grids,<sup>3</sup> molecular cylinders,<sup>4</sup> and three-dimensional cages.<sup>5</sup> Among the metal-containing organic supramolecular systems, molecular squares produced from metallocorners and linear bridging ligands have attracted special interests due to not only their convenient

preparation and reliable characterization but also their useful applications in molecular recognition,<sup>6</sup> catalysis,<sup>7</sup> electrochemical sensing,<sup>8</sup> photoluminescence,<sup>9</sup> and so forth.

The desired functionality in metallosupramolecular squares

- (1) For recent comprehensive reviews, see: (a) Leininger, S.; Olenyuk, B.; Stang, P. J. *Chem. Rev.* **2000**, *100*, 853–908. (b) Swiegers, G. F.; Malefetse, T. J. *Chem. Rev.* **2000**, *100*, 3483–3537. (c) Holliday, B. J.; Mirkin, C. A. *Angew. Chem., Int. Ed.* **2001**, *40*, 2022–2043.
- (2) (a) Archer, R. D. *Coord. Chem. Rev.* **1993**, *128*, 49–68. (b) Brunsveld, L.; Folmer, B. J. B.; Meijer, E. W.; Sijbesma, R. P. *Chem. Rev.* **2001**, *101*, 4071–4097. (c) Michelsen, U.; Hunter, C. A. *Angew. Chem., Int. Ed.* **2000**, *29*, 764–767. (d) Dobrawa, R.; Würthner, F. *Chem. Commun.* **2002**, 1878–1879. (e) Ayabe, M.; Yamashita, K.; Sada, K.; Shinkai, S.; Ikeda, A.; Sakamoto, S.; Yamaguchi, K. *J. Org. Chem.* **2003**, *68*, 1059–1066.
- (3) (a) Baxter, P. N. W.; Lehn, J.-M.; Fischer, J.; Youinou, M.-T. *Angew. Chem., Int. Ed. Engl.* **1994**, *33*, 2284–2287. (b) Bassani, D. M.; Lehn, J.-M.; Fromm, K.; Fenske, D. *Angew. Chem., Int. Ed.* **1998**, *37*, 2364–2367. (c) Ziener, U.; Lehn, J.-M.; Mourran, A.; Möller, M. *Chem.—Eur. J.* **2002**, *8*, 951–957. (d) Marquis, A.; Kintzinger, J.-P.; Graff, R.; Baxter, P. N. W.; Lehn, J.-M. *Angew. Chem., Int. Ed.* **2002**, *41*, 2760–2764.
- (4) (a) Stang, P. J.; Olenyuk, B. *Acc. Chem. Res.* **1997**, *30*, 502–518. (b) Mamula, O.; von Zelewsky, A.; Bernardinelli, G. *Angew. Chem., Int. Ed.* **1998**, *37*, 289–293. (c) Schnebeck, R.-D.; Freisinger, E.; Glahe, F.; Lippert, B. *J. Am. Chem. Soc.* **2000**, *122*, 1381–1390. (d) Yamanoi, Y.; Sakamoto, Y.; Kusakawa, T.; Fujita, M.; Sakamoto, S.; Yamaguchi, K. *J. Am. Chem. Soc.* **2001**, *123*, 980–981. (e) Takahashi, R.; Kobuke, Y. *J. Am. Chem. Soc.* **2003**, *125*, 2372–2373.
- (5) (a) Fujita, M.; Yu, S.-Y.; Kusakawa, T.; Funaki, H.; Ogura, K.; Yamaguchi, K. *Angew. Chem., Int. Ed.* **1998**, *37*, 2082–2085. (b) Caulder, D. L.; Powers, R. E.; Parac, T. N.; Raymond, K. N. *Angew. Chem., Int. Ed.* **1998**, *37*, 1840–1843. (c) Fochi, F.; Jacopozzi, P.; Wegelius, E.; Rissanen, K.; Cozzini, P.; Marastoni, E.; Fiscaro, E.; Manini, P.; Fokkens, R.; Dalcanales, E. *J. Am. Chem. Soc.* **2001**, *123*, 7539–7552. (d) Saalfrank, R. W.; Glaser, H.; Demleiter, B.; Hampel, F.; Chowdhry, M. M.; Schünemann, V.; Trautwein, A. X.; Vaughan, G. B. M.; Yeh, R.; Davis, A. V.; Raymond, K. N. *Chem.—Eur. J.* **2002**, *8*, 493–497. (e) Kusakawa, T.; Fujita, M. *J. Am. Chem. Soc.* **2002**, *124*, 13576–13582. (f) Pironcini, L.; Bertolini, F.; Cantadori, B.; Ugozzoli, F.; Massera, C.; Dalcanales, E. *Proc. Natl. Acad. Sci. U.S.A.* **2002**, *99*, 4911–4915. (g) Tsuda, A.; Nakamura, T.; Sakamoto, S.; Yamaguchi, K.; Osuka, A. *Angew. Chem., Int. Ed.* **2002**, *41*, 2817–2821. (h) Seidel, S. R.; Stang, P. J. *Acc. Chem. Res.* **2002**, *35*, 972–983.
- (6) (a) Fujita, M.; Yazaki, J.; Ogura, K. *J. Am. Chem. Soc.* **1990**, *112*, 5645–5647. (b) Dinolfo, P. H.; Hupp, J. T. *Chem. Mater.* **2001**, *13*, 3113–3125. (c) Müller, C.; Whiteford, J. A.; Stang, P. J. *J. Am. Chem. Soc.* **1998**, *120*, 9827–9837. (d) Jeong, K.-S.; Cho, Y. L.; Song, J. U.; Chang, H.-Y.; Choi, M.-G. *J. Am. Chem. Soc.* **1998**, *120*, 10982–10983. (e) Jeong, K.-S.; Cho, Y. L.; Chang, S.-Y.; Park, T.-Y.; Song, J. U. *J. Org. Chem.* **1999**, *64*, 9459–9466. (f) Lee, S. J.; Lin, W. *J. Am. Chem. Soc.* **2002**, *124*, 4554–4555.
- (7) (a) Slone, R. V.; Benkstein, K. D.; Bélanger, S.; Hupp, J. T.; Guzei, I. A.; Rheingold, A. L. *Coord. Chem. Rev.* **1998**, *171*, 221–243. (b) Merlau, M. L.; Mejia, M. P.; Nguyen, S. T.; Hupp, J. T. *Angew. Chem., Int. Ed.* **2001**, *40*, 4239–4242.
- (8) (a) Lahav, M.; Gabai, R.; Shipway, A. N.; Willner, I. *Chem. Commun.* **1999**, 1937–1938. (b) Shipway, A. N.; Katz, E.; Willner, I. *ChemPhysChem* **2000**, *1*, 18–52. (c) Cotton, F. A.; Daniels, L. M.; Lin, C.; Murillo, C. A. *J. Am. Chem. Soc.* **1999**, *121*, 4538–4539. (d) Cotton, F. A.; Lin, C.; Murillo, C. A. *J. Am. Chem. Soc.* **2001**, *123*, 2670–2671.
- (9) (a) Slone, R. V.; Yoon, D. I.; Calhoun, R. M.; Hupp, J. T. *J. Am. Chem. Soc.* **1995**, *117*, 11813–11814. (b) Fan, J.; Whiteford, J. A.; Olenyuk, B.; Levin, M. D.; Stang, P. J.; Fleischer, E. B. *J. Am. Chem. Soc.* **1999**, *121*, 2741–2752. (c) Sun, S.-S.; Lees, A. J. *Inorg. Chem.* **2001**, *40*, 3154–3160.

may be introduced by employing functional ligands or properly functionalized metal corners with appropriate size and shape. To date, considerable efforts have been devoted to the design and preparation of metal corners, and various functional metal corners that contain crown ether,<sup>10</sup> calixarene,<sup>10</sup> and ferrocene<sup>11</sup> have been successfully used to provide the respective metallo-supramolecular squares with organic ligands. In contrast to the functional metal corners, only few functional bridging ligands have been reported so far; for example, ditopic porphyrins<sup>9b,12</sup> have been used as bridging ligands for photochemically active metallosupramolecular squares.

Recently, we have successfully prepared molecular squares with a perylene skeleton, which exhibited excellent fluorescence properties with quantum yield of almost unity.<sup>13</sup> Attractive opportunities exist to introduce functional groups into the bay positions of perylene<sup>13c</sup> to provide bridging ligands for functional square assemblies. In this regard, the question arises whether, by introducing electrochemically active groups into perylene-based bridging ligands, supramolecular squares with novel electrochemical properties may be accessible. As a stable and reversibly oxidizable functional organometallic complex, ferrocene has been widely used as a redox active building block in supramolecular chemistry and representatively served as the core<sup>14</sup> or the peripheral moiety<sup>15,16</sup> in metallodendrimers. Also molecular squares in which ferrocenes are positioned at the metal corners,<sup>11</sup> or as linkers,<sup>17</sup> have been reported. However, functional metallosupramolecular squares containing multiple ferrocenes in bridging ligands are unknown to date. In the present work, we report on the amplification of a redox functionality with a factor of  $4 \times 4 = 16$ , which equals to  $2^4$  in conventional dendrimer chemistry, by self-assembly of 4-fold ferrocene-substituted perylene bisimide dyes with Pt(II) phosphine corner to supramolecular squares. Furthermore, the redox properties of free ligands and the corresponding square assemblies have been studied in detail by cyclic voltammetry, spectroelectrochemistry, and redox titration as well.

## Results and Discussion

**Synthesis of Ferrocenyl-Substituted Perylene Bisimides.** Ferrocenyl-substituted *N,N'*-di(4-pyridyl)perylene bisimide ditopic ligands **4a** and **4b** were synthesized according to Scheme 1 in three steps starting from tetra(4-butoxyphenoxy)perylene bisanhydride **1**.<sup>18</sup> In the first step, perylene bisanhydride **1** was converted to the bisimide derivative **2** by imidization with 4-aminopyridine in quinoline in the presence of catalytic amounts of zinc acetate. Subsequently, the butyl ether groups were cleaved by  $\text{BBr}_3$  to give tetra(4-hydroxyphenoxy)perylene bisimide **3**. The esterification of phenolic groups in substrate **3** with ferrocenylbutyric acid and ferrocenylvaleric acid through activation of the carboxylic acid function by dicyclohexylcarbodiimide (DCC) in the presence of dimethylaminopyridinium toluenesulfonate (DPTS)<sup>19</sup> afforded the corresponding ferrocenyl-substituted *N,N'*-di(4-pyridyl)perylene bisimide ligands **4a** and **4b** in moderate yields.

For comparison purposes, the ferrocenyl-substituted *N,N'*-di-(2,6-diisopropylphenyl)perylene bisimides **8a,b** were prepared as reference compounds from perylene bisimide **6** according to the procedures applied for ligands **4a,b** by  $\text{BBr}_3$ -promoted ether cleavage and subsequent esterification (Scheme 2). The 4-butoxyphenoxy perylene bisimide **6** was prepared in turn by the nucleophilic substitution of the corresponding tetrachloro precursor **5**<sup>20</sup> with 4-butoxyphenol in *N*-methylpyrrolidone (NMP) in the presence of potassium carbonate. The hitherto unknown dipyriddy ligands **4** and their reference compounds **8** were fully characterized by <sup>1</sup>H NMR and MALDI-TOF mass spectroscopy and elemental analyses as well (see Experimental Section).

**Self-Assembly of Metallosupramolecular Squares.** The metal complex  $[\text{Pt}(\text{dppp})][(\text{OTf})_2]$  (dppp = 1,3-bis(diphenylphosphano)propane; OTf = trifluoromethanesulfonate) has been known to be a versatile 90° corner for the construction of square supramolecular assemblies with linear bridging ligands.<sup>21</sup> Therefore, this Pt(II) complex was chosen as an angular building block for the metal-mediated self-assembly of newly prepared ferrocene-functionalized ditopic perylene ligands **4**. Indeed, the treatment of  $[\text{Pt}(\text{dppp})][(\text{OTf})_2]$  with equimolar amounts of ligand **4a** or **4b** in dichloromethane at room temperature formed quantitatively the corresponding molecular squares **9a** and **9b** (Scheme 3). Subsequent precipitation with diethyl ether afforded the analytically pure squares **9a** and **9b** in 68% and 77% yield.

Besides elemental analysis, NMR studies of the isolated products suggest the formation of uniform macrocyclic complexes through coordination of perylene ligands **4** with Pt(II) phosphine corner. As demanded by their highly symmetric geometry, both squares **9a** and **9b** display in <sup>31</sup>P{<sup>1</sup>H} NMR spectra a sharp singlet with appropriate <sup>195</sup>Pt satellites<sup>21</sup> for the equivalent phosphorus atoms. The fact that the <sup>31</sup>P signals are shifted upfield by 8.5 ppm relative to that of the precursor complex  $[\text{Pt}(\text{dppp})][(\text{OTf})_2]$  provides evidence for the ligation of Pt(dppp) with 4-pyridine receptors in ligands **4a,b**. The <sup>1</sup>H NMR spectra of squares **9a,b** show only a single set of signals for the ligands and the dppp moieties with significant downfield

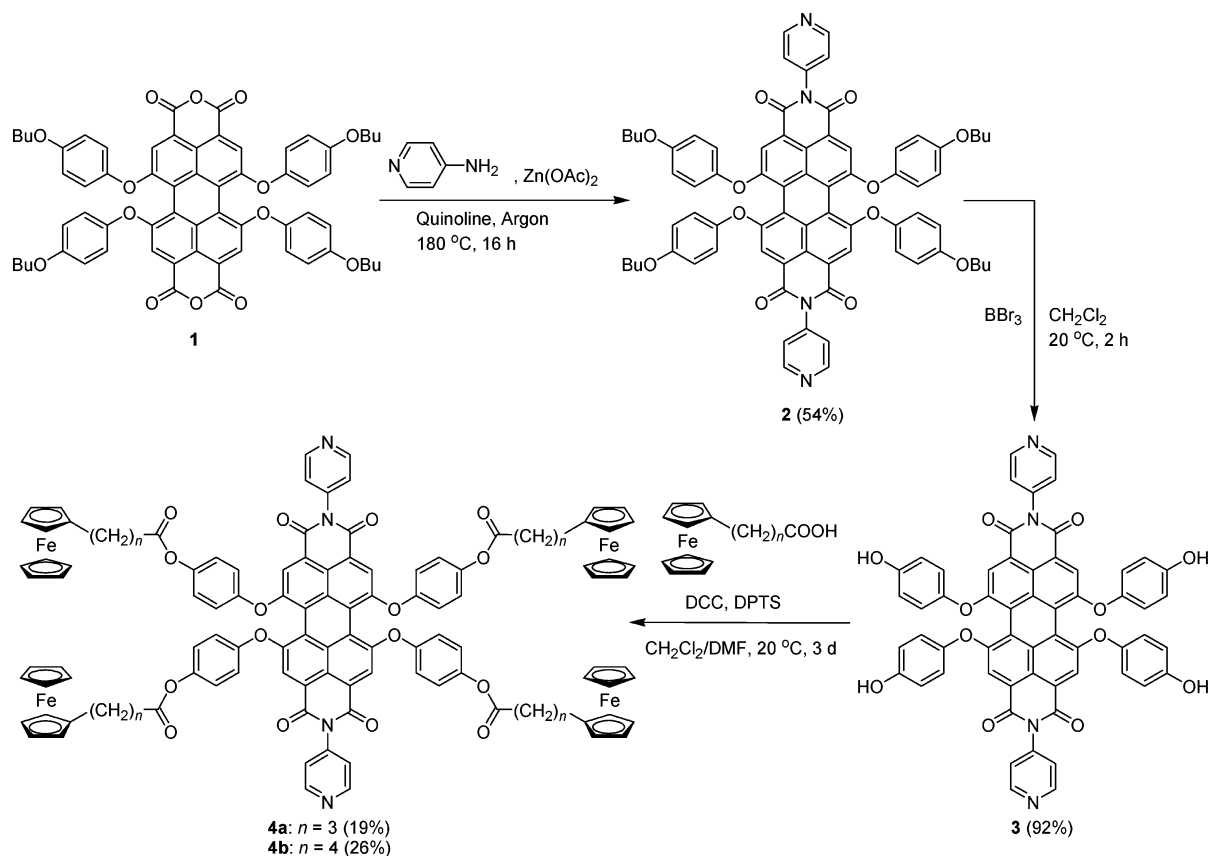
- (10) Stang, P. J.; Cao, D. H.; Chen, K.; Gray, G. M.; Muddiman, D. C.; Smith, R. D. *J. Am. Chem. Soc.* **1997**, *119*, 5163–5168.  
 (11) (a) Stang, P. J.; Olenyuk, B.; Fan, J.; Arif, A. M. *Organometallics* **1996**, *15*, 904–908. (b) Sun, S.-S.; Anspach, J. A.; Lees, A. J. *Inorg. Chem.* **2002**, *41*, 1862–1869.  
 (12) (a) Drain, C. M.; Lehn, J.-M. *J. Chem. Soc., Chem. Commun.* **1994**, 2313–2315. (b) Stone, R. V.; Hupp, J. T. *Inorg. Chem.* **1997**, *36*, 5422–5423. (c) Jengo, E.; Milani, B.; Zangrando, E.; Geremia, S.; Alessio, E. *Angew. Chem., Int. Ed.* **2000**, *39*, 1096–1099.  
 (13) (a) Würthner, F.; Sautter, A. *Chem. Commun.* **2000**, 445–446. (b) Würthner, F.; Sautter, A.; Schmid, D.; Weber, P. J. A. *Chem.—Eur. J.* **2001**, *7*, 894–902. (c) Würthner, F.; Sautter, A. *Org. Biomol. Chem.* **2003**, *1*, 240–243.  
 (14) (a) Cardona, C. M.; Kaifer, A. E. *J. Am. Chem. Soc.* **1998**, *120*, 4023–4024. (b) Cardona, C. M.; McCarley, T. D.; Kaifer, A. E. *J. Org. Chem.* **2000**, *65*, 1857–1864. (c) Stone, D. L.; Smith, D. K.; McGrail, P. T. *J. Am. Chem. Soc.* **2002**, *124*, 856–864. (d) Ashton, P. R.; Balzani, V.; Clemente-León, M.; Colonna, B.; Credi, A.; Jayaraman, N.; Raymo, F. M.; Stoddart, J. F.; Venturi, M. *Chem.—Eur. J.* **2002**, *8*, 673–684.  
 (15) (a) Fillaut, J.-L.; Astruc, D. *J. Chem. Soc., Chem. Commun.* **1993**, 1320–1322. (b) Fillaut, J.-L.; Linares, J.; Astruc, D. *Angew. Chem., Int. Ed. Engl.* **1994**, *33*, 2460–2462. (c) Shu, C.-F.; Shen, H.-M. *J. Mater. Chem.* **1997**, *7*, 47–52. (d) Deschenaux, R.; Serrano, E.; Levelut, A. M. *Chem. Commun.* **1997**, 1577–1578. (e) Valério, C.; Fillaut, J.-L.; Ruiz, J.; Guittard, J.; Blais, J.-C.; Astruc, D. *J. Am. Chem. Soc.* **1997**, *119*, 2588–2589. (f) Köllner, C.; Pugin, B.; Togni, A. *J. Am. Chem. Soc.* **1998**, *120*, 10274–10275. (g) Ipaktschi, J.; Hosseinzadeh, R.; Schlaf, P. *Angew. Chem., Int. Ed.* **1999**, *38*, 1658–1660. (h) Alvarez, J.; Ren, T.; Kaifer, A. E. *Organometallics* **2001**, *20*, 3543–3549.  
 (16) (a) Alonso, B.; Cuadrado, I.; Morán, M.; Losada, J. J. *J. Chem. Soc., Chem. Commun.* **1994**, 2575–2576. (b) Cuadrado, I.; Morán, M.; Casado, C. M.; Alonso, B.; Lobete, F.; Garcia, B.; Ibisate, M.; Losada, J. *Organometallics* **1996**, *15*, 5278–5280. (c) Cuadrado, I.; Casado, C. M.; Alonso, B.; Morán, M.; Losada, J.; Belsky, V. *J. Am. Chem. Soc.* **1997**, *119*, 7613–7614. (d) Casado, C. M.; González, B.; Cuadrado, I.; Alonso, B.; Morán, M.; Losada, J. *Angew. Chem., Int. Ed.* **2000**, *39*, 2135–2138.  
 (17) Cotton, F. A.; Lin, C.; Murillo, C. A. *Acc. Chem. Res.* **2001**, *34*, 759–771.

(18) Schneider, M.; Müllen, K. *Chem. Mater.* **2000**, *12*, 352–362.

(19) Moore, J. S.; Stupp, S. I. *Macromolecules* **1990**, *23*, 65–70.

(20) (a) Seybold, G.; Wagenblast, G. *Dyes Pigm.* **1989**, *11*, 303–317. (b) Klok, H.-A.; Hernández, J. R.; Becker, S.; Müllen, K. *J. Polym. Sci., Part A: Polym. Chem.* **2001**, *39*, 1572–1583.

(21) Stang, P. J.; Cao, D. H.; Saito, S.; Arif, A. M. *J. Am. Chem. Soc.* **1995**, *117*, 6273–6283.

**Scheme 1.** Synthesis of Ferrocenyl-Substituted *N,N'*-Di(4-pyridyl)perylene Bisimide Ligands **4**

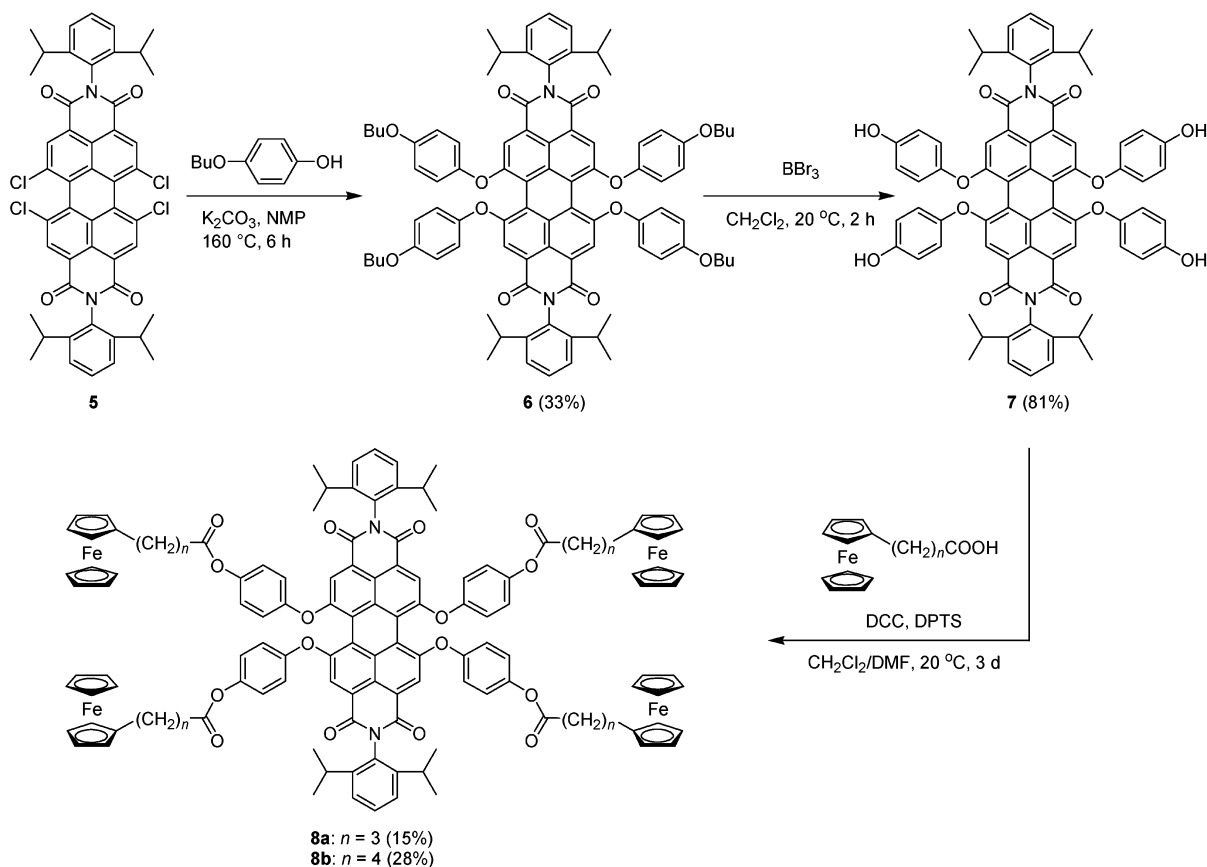
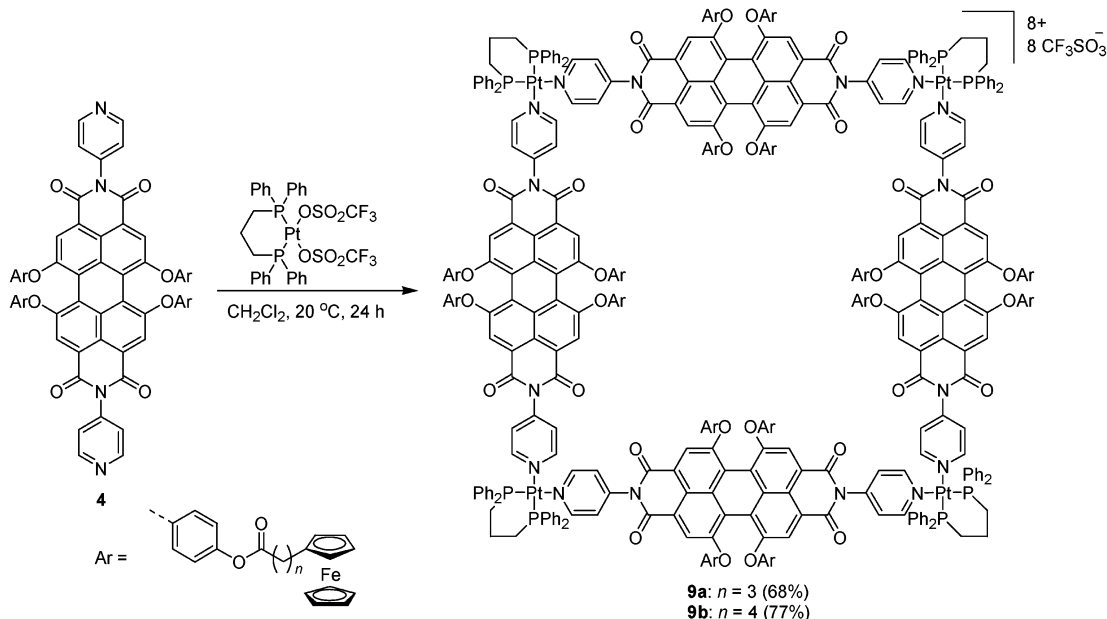
shifts ( $\Delta\delta = 0.35$  ppm) of the  $\alpha$ -pyridyl protons compared to that of free ligands owing to the metal complexation. Upon formation of the supramolecular structure, the  $^1\text{H}$  NMR signals of ferrocenyl groups were broadened to a single signal with a slight downfield shift (see Figures S1 and S2 in the Supporting Information). Variable temperature  $^1\text{H}$  NMR studies showed that at lower temperature (278 K) the proton signals are more broadened, while the signals become notably sharp at higher temperature (328 K). Because no concentration dependence was observed in  $^1\text{H}$  NMR measurements, the signal broadening is not due to some complex association/dissociation processes but rather is caused by rotational hindrance of the perylene bisimide moiety imposed by ferrocenyl substituents in molecular squares. Furthermore, both complexes **9a,b** remain highly soluble in dichloromethane, chloroform, nitromethane, and similar organic solvents, despite their high molecular weights (over 11 000 Da) and charges, which is in agreement with the presence of well-defined assemblies rather than linear oligomeric products.

**Optical Properties of Squares 9.** The optical properties of the ferrocene-containing molecular squares **9a,b** were investigated by UV/vis spectroscopy and fluorescence measurements. The UV/vis spectra of these squares in dichloromethane exhibit intense absorption bands with maxima at 579, 543, and 452 nm, which are characteristic for the perylene bisimide chromophore.<sup>13b</sup> Compared with the corresponding free ligands **4a,b**, the absorption maxima of **9a,b** are bathochromically shifted by about 5 nm (see Figures S6 and S7 in the Supporting Information), suggesting coordination of the 4-pyridine group to Pt(II). As expected, the weak absorption of ferrocene around 440 nm ( $\epsilon = 91 \text{ dm}^3 \text{ mol}^{-1} \text{ cm}^{-1}$ ) is hidden by overlapping of the strong absorption band of perylene. Ferrocenyl substituents

in **4** and **9** did not affect the absorption properties of the perylene bisimide chromophore, and no additional bands due to charge transfer were observed, implying that insignificant or no ground-state electronic interaction between these two chromophores exists.

In contrast to absorption properties, fluorescence properties of the perylene bisimide chromophore are strongly affected by the presence of ferrocenyl substituents. Alkylphenoxy perylene bisimide ligands and their Pt(II) squares possess high fluorescence quantum yields ( $\Phi_{\text{F}} = 0.86\text{--}0.94$ )<sup>13b</sup> in chloroform or dichloromethane, while the ferrocene-substituted perylene bisimide ligands **4a,b** and the corresponding squares **9a,b** are poor fluorescent ( $\Phi_{\text{F}} < 0.002$ ) in dichloromethane. The low fluorescence quantum yields of the present compounds are presumably due to the deactivation of the photoexcited singlet state of perylene bisimide through reductive electron transfer from ferrocenes, which is supported by the following facts: For these ferrocene-containing perylene bisimides, the energy level of the charge-separated state (perylene<sup>•-</sup>-Fc<sup>•+</sup>) is about 1 eV, as calculated from cyclic voltammetric reduction and oxidation potentials (see next section). Because the lowest singlet-excited state of these perylene bisimides lies ca. 2.15 eV above the ground state, the photoinduced intramolecular electron-transfer reaction is exothermic by ca. 1.15 eV (110 kJ mol<sup>-1</sup>) and, therefore, thermodynamically feasible. On the other hand, the singlet-excited state of ferrocene (2.46 eV)<sup>22</sup> is above that of the perylene chromophore (2.15 eV), thus, quenching by the perylene $\rightarrow$ ferrocene energy transfer would be forbidden due to

(22) (a) Giasson, R.; Lee, E. J.; Zhao, X.; Wrighton, M. S. *J. Phys. Chem.* **1993**, *97*, 2596–2601. (b) Thornton, N. B.; Wojtowicz, H.; Netzel, T.; Dixon, D. W. *J. Phys. Chem. B* **1998**, *102*, 2101–2110.

**Scheme 2.** Synthesis of Ferrocenyl-Substituted *N,N'*-Di(2,6-diisopropylphenyl)perylene Bisimides **8****Scheme 3.** Self-Assembly of Metallosupramolecular Squares **9**

the endothermic effect by 0.31 eV ( $30\text{ kJ mol}^{-1}$ ). In fact, it has been reported that covalently linked ferrocenes substantially quenched the fluorescence emission of other chromophores, for example, porphyrins, through an intramolecular electron-transfer process.<sup>22</sup>

#### Electrochemical Properties of Perylene Bisimide Ligands.

To assess the effect of redox active ferrocenes on the electrochemical properties of perylene bisimide core, first the ferrocene-

containing ligands **4a,b** and their reference compounds **8a,b** were investigated by cyclic voltammetry in dichloromethane. The cyclic voltammograms of **4a** and **8a** are shown in Figure 1. The cyclic voltammogram of the ferrocene-functionalized perylene bisimide ligand **4a** (Figure 1a) shows two reversible reduction waves at  $E_{1/2} = -1.00$  and  $-1.16$  V (versus  $\text{Fc}/\text{Fc}^+$ ) and a 4 times larger reversible oxidation wave at  $E_{1/2} = -0.01$  V (versus  $\text{Fc}/\text{Fc}^+$ ). The two reduction waves are comparable to

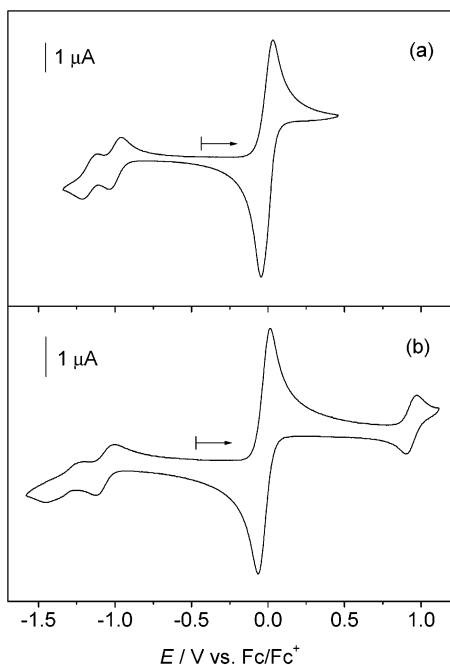


**Figure 1.** Cyclic voltammograms of perylene bisimides **4a** (a) and **8a** (b) in  $\text{CH}_2\text{Cl}_2$ , sweep rate  $100 \text{ mV s}^{-1}$ .

those of *tert*-butylphenoxy perylene bisimide,<sup>13b</sup> which bears no ferrocene units in the molecule, indicating that ferrocenyl substituents tethered by flexible propyl chains do not influence the reduction process of the perylene bisimide moiety. The wave observed in the oxidation cycle ( $E_{1/2} = -0.01 \text{ V}$ ) should be ascribed to the oxidation of four ferrocenyl groups. Further oxidation of ligand **4a** is irreversible, which is attributed to the oxidation of perylene bisimide involving the lone pairs of pyridyl nitrogen atoms. As known from our earlier studies, this process causes adsorption of the ligand on the platinum electrode.<sup>13b</sup> Similar electrochemical properties were observed for the ligand **4b** where the ferrocenes are tethered to the perylene core by butyl chains. While the extended oxidation of pyridyl ligands **4a,b** is irreversible, the reference compound **8a** (Figure 1b), in which *N*-pyridine is replaced by a *N*-phenyl group, shows a reversible wave at  $E_{1/2} = +0.93 \text{ V}$  for the oxidation of perylene bisimide, in addition to the two reversible reductions at  $E_{1/2} = -1.06$  and  $-1.32 \text{ V}$  and the reversible oxidation at  $E_{1/2} = -0.03 \text{ V}$ . Clearly, the replacement of nitrogen atoms by carbon atoms avoids the adsorption of **8a** on the platinum working electrode; thus, the oxidation of perylene core in **8**, in contrast to **4**, becomes reversible.

To obtain further insight into the redox processes of ferrocene-functionalized perylene bisimides, spectroelectrochemistry of ligand **4b** was studied by recording its UV/vis–NIR absorption spectra in dichloromethane at different reduction potentials (Figure 2). Once the applied potential approached the first reduction potential of **4b**, the UV/vis absorption bands of the neutral species **4b** (447, 537 and 575 nm) essentially disappeared, while new absorption bands appeared in the NIR region, one very intense at 784 nm and two weak transitions at 969 and 1073 nm (Figure 2a). These new bands may be attributed to the generation of radical anionic species  $\mathbf{4b}^{\bullet-}$ . When the potential was increased to the second reduction process, the absorption bands of  $\mathbf{4b}^{\bullet-}$  were completely diminished, accompanied by the appearance of a broad absorption band with

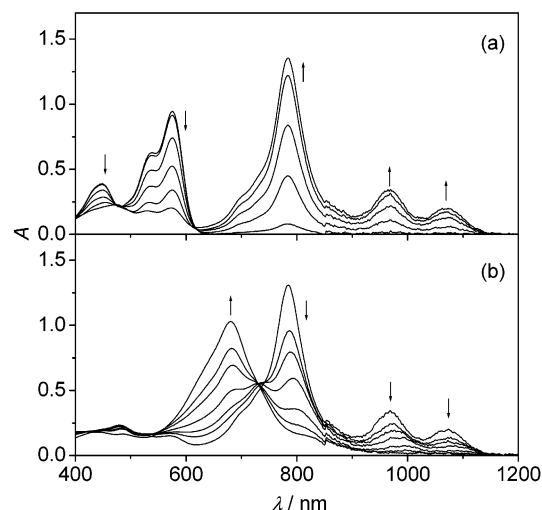


**Figure 2.** Spectroelectrograms of perylene bisimide ligand **4b** in  $\text{CH}_2\text{Cl}_2$ . Stepwise increasing of the applied potential to (a) the first reduction (radical anionic perylene bisimide species) and (b) the second reduction of **4b** (dianionic perylene bisimide species).

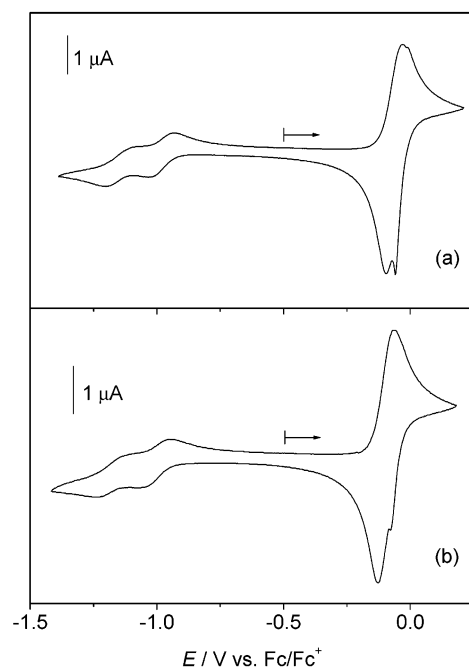


**Figure 3.** Cyclic voltammograms of metallocsupramolecular squares **9a** (a) and **9b** (b) in  $\text{CH}_2\text{Cl}_2$ , sweep rate  $100 \text{ mV s}^{-1}$ .

a maximum at 680 nm (Figure 2b), which is characteristic for perylene bisimide dianionic species.<sup>13b</sup> These spectroelectrochemical results imply that **4b** was reduced by two one-electron reductions through its radical anionic states  $\mathbf{4b}^{\bullet-}$  to the dianionic species  $\mathbf{4b}^{2-}$ .

**Electrochemical Properties of Metallocsupramolecular Squares 9.** Once the electrochemical features of ferrocene-containing free ligands **4** were assessed, the 16-fold ferrocenyl-substituted molecular squares **9** were investigated by cyclic voltammetry to elucidate a supramolecular effects on redox processes. The cyclic voltammogram of square **9a** in dichloromethane (Figure 3a) shows two reversible reduction waves ( $E_{1/2} = -0.98$  and  $-1.13 \text{ V}$ ). Since similar waves were observed for the free ligands **4** and their reference compounds **8**, these reversible waves should also be assigned to the reduction of

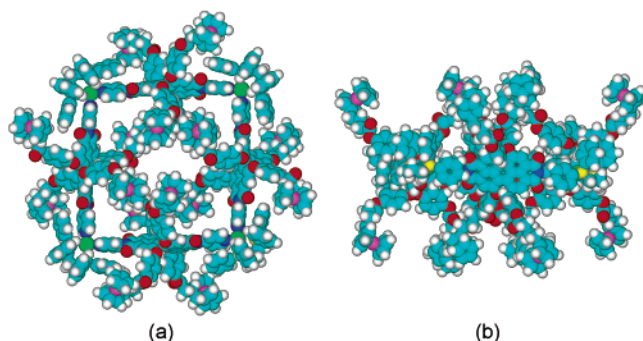


**Figure 4.** Top (a) and side (b) views of energy minimized structures of molecular square **9a**.

the perylene bisimide skeleton. Interestingly, for the ferrocenium groups in **9a**, peak splitting was observed at  $E = -0.06$  and  $-0.10$  V for the reductive wave and a shoulder was observed at  $E = -0.01$  V for the oxidative wave. As such a peak splitting was not observed for the corresponding free ligand **4a**, this electrochemical property pinpoints a supramolecular effect. The square **9b** exhibits similar electrochemical behavior (Figure 3b). Two “normal” reversible waves ( $E_{1/2} = -1.01$  and  $-1.18$  V) were observed for the perylene bisimide reduction and peak splitting, however, somewhat less pronounced, appeared during the reduction of ferroceniums at  $E = -0.13$  V and a shoulder appeared at  $E = -0.08$  V, in contrast to the one anodic peak at  $E = -0.07$  V for the oxidation of ferrocenes.

To understand the observed supramolecular effect on the reduction process of ferrocenium groups, pertinent structural features of squares **9** have to be discussed. X-ray analysis and molecular modeling results revealed that the four substituents at the 1,6,7,12-positions (bay area) of perylene bisimides lead to two naphthalene imide half units twisted by ca.  $30^\circ$ .<sup>23</sup> The twisted conformation entails that when ligands **4a** or **4b** is self-assembled to a square scaffold, the 16 ferrocene units should be separated into two groups: one set is pointed toward the inside of the square cavity, while the other set orients outside. Indeed, molecular dynamic simulation of square **9a** confirms these structural features (Figure 4). The neutral ferrocene units are conformationally still flexible due to the presence of an alkyl linkage; therefore, their oxidation to ferrocenium may not be affected by the supramolecular organization. However, the conformation and flexibility of ferroceniums, which are generated through the one-electron oxidation of ferrocenes, will be critically restricted because of the electrostatic repulsion between the adjacent ferrocenium units. The ferrocenium moieties inside the square are located in a more hydrophobic microenvironment than the outside ferrocenium groups. Thus, latter ones may be stabilized by the bulky polar electrolyte, while the inside ferroceniums are not easily accessible by the polar electrolyte and, therefore, less stable.<sup>24</sup> In addition, the eight counterions for the four positively charged platinum centers would occupy at least partially the square cavity, which also prevents the inside ferroceniums from being stabilized by external counterions.

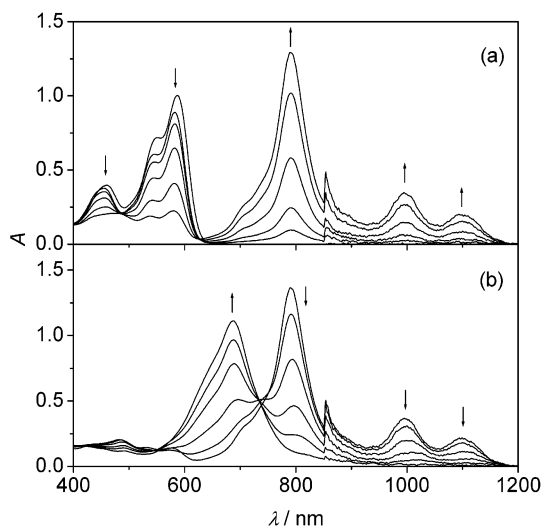


**Figure 5.** Spectroelectrograms of metallasupramolecular square **9b** in  $\text{CH}_2\text{-Cl}_2$ . Stepwise increasing of the applied potential to (a) the first reduction (radical anionic perylene bisimide species) and (b) the second reduction of **9b** (dianionic perylene bisimide species).

Consequently, the inside ferroceniums should be more easily reduced to ferrocene than the outside ones, i.e., exhibit a higher  $E_{1/2}$  value. As a result, two peaks are expected in the reduction cycle of ferroceniums, which were indeed observed in the cyclic voltammograms of squares **9** (Figure 3). This interpretation is also corroborated by the unusual shape of the cyclic voltammogram with a very sharp first reduction peak that points on different kinetics for the two reduction steps. Thus, while the inner ferrocenium ions are expected to be easier to reduce from the thermodynamic point of view, the outer ones are at a close distance to the electrode leading to faster kinetics. A similar behavior was observed by Heinze et al. in the cyclic voltammetric study on the two-step oxidation of 5,6-dimethyl-5,6-dihydrobenzo[*c*]cinnoline and called the “spike effect”.<sup>25</sup>

To obtain more information on the redox process, spectroelectrochemical investigations of metallasupramolecular square **9b** were carried out. The successive increase of applied potential up to the first reduction potential of square **9b** resulted in the disappearance of the UV/vis absorption bands of **9b** (452, 543, and 579 nm), while three new absorption bands (789, 994, and 1093 nm) appeared in the NIR region (Figure 5a). Since identical spectral changes were observed for the ligand **4b**, these new UV/vis–NIR absorptions are assigned to the perylene bisimide radical anion. Once the applied potential was further increased to the second reduction potential of **9b**, the absorption bands for the radical anionic species were diminished and a new broad band for perylene bisimide dianionic species appeared at 688 nm (Figure 5b), as in the case of ligand **4b**. These results imply that a similar mechanism applies for the reduction of free ligand **4b** and metallasupramolecular square **9b** and that all of perylene bisimides in the square assembly are reduced to the radical anions and the dianions at the respective potentials.

It has been reported that a reversible oxidation wave of the tetraphenoxyperylene bisimide unit is observable at about 1 V for simple perylene bispyridyl squares when the nitrogen lone pairs are blocked by platinum coordination.<sup>13b</sup> By contrast, at ca. 1 V the oxidation of squares **9a** and **9b** remains irreversible,

(23) (a) Würthner, F.; Sautter, A.; Thalacker, C. *Angew. Chem., Int. Ed.* **2000**, *39*, 1243–1245. (b) Hofkens, J.; Vosch, T.; Maus, M.; Köhn, F.; Cotlet, M.; Weil, T.; Herrmann, A.; Müllen, K.; De Schryver, F. C. *Chem. Phys. Lett.* **2001**, *333*, 255–263.

(24) (a) Pochapsky, S. S.; Mo, H.; Pochapsky, T. C. *J. Chem. Soc., Chem. Commun.* **1995**, 2513–2514. (b) Beer, P. D.; Graydon, A. R.; Johnson, A. O. M.; Smith, D. K. *Inorg. Chem.* **1997**, *36*, 2112–2118.

(25) Dietrich, M.; Heinze, J.; Krieger, C.; Neugebauer, F. A. *J. Am. Chem. Soc.* **1996**, *118*, 5020–5030.

which suggests that ferrocene-functionalized self-assembled squares are less stable than the previously reported perylene bisimide-based squares.<sup>13b</sup> The major difference between these two perylene bisimide derived molecular squares is that **9a,b** are already highly charged species at the given voltage due to the ferrocenium units. According to Figure 3, all 16 ferrocene groups in squares **9** are transformed to ferroceniums at ca. 0 V to generate supramolecular structures with a total of 24 positive charges (8 at Pt(II) and 16 by ferrocene one-electron oxidations). In these highly charged and sterically crowded structures, the Coulombic repulsion between adjacent ferrocenium groups will destabilize the assemblies. As a consequence, upon further oxidation the molecular squares may decompose through rupture of metal–ligand bonds to form linear oligomeric chains. Indeed, the characteristic peak split around the redox wave of ferrocene subunits in the back scan (Figure 3) disappeared after further oxidation, indicating the loss of the supramolecular effect.

**Chemical Oxidation of Ferrocene-Functionalized Perylene Bisimides and Molecular Squares.** Our electrochemical and spectroelectrochemical studies revealed that all 16 ferrocenyl groups in molecular squares **9a,b** may be oxidized by the one-electron oxidation process to generate highly charged species. However, in contrast to the pronounced spectral changes observed for the perylene bisimides upon reduction (Figures 2 and 5), little spectral changes could be seen upon ferrocene oxidation owing to the much stronger absorbance of the perylene chromophores. To shed more light on this oxidation process, we have extended our investigation to chemical oxidation of the ferrocene-substituted ditopic ligand **4b** and its square assembly **9b** by the thianthrene radical cation ( $\text{Th}^+$ ), a well-established one-electron oxidant.<sup>26</sup> The reduction potential of  $\text{Th}^+$  was determined to be about  $E_{1/2} = +0.85$  V versus  $\text{Fc}/\text{Fc}^+$  couple in dichloromethane (literature value, 1.10 V versus SCE in acetonitrile<sup>27</sup>); thus,  $\text{Th}^+$  should easily oxidize ferrocenyl moieties ( $E_{1/2} = 0.0$  V) and partly oxidize the perylene core ( $E_{1/2} = +0.93$  V).

The thianthrene radical cation shows a major UV/vis absorption at around 550 nm, which disappears upon accepting one electron to give neutral thianthrene; the latter one has no absorption over 300 nm. Therefore, the redox process may be easily monitored by UV/vis spectroscopy. To examine this possibility, the redox titration of the model compound 5-ferrocenylpentanoic acid 4-methoxyphenyl ester (**10**) with thianthrenium pentachloroantimonate was investigated by UV/vis spectroscopy (Figure 6). Upon addition of the oxidant to the solution of **10**, two absorption bands, an intense one at 365 nm and a broad weak one at around 630 nm, appeared due to the oxidation of the ferrocenyl moiety to ferrocenium.<sup>28</sup> The latter one is responsible for the characteristic blue color of ferrocenium ions. The intensities of these absorptions increased steadily with the increasing amount of  $\text{Th}^+$  until a 1:1 stoichiometry of  $\text{Th}^+:\mathbf{10}$  was achieved (Figure 6, inset). The characteristic absorption of  $\text{Th}^+$  became visible at 550 nm when an excess amount of

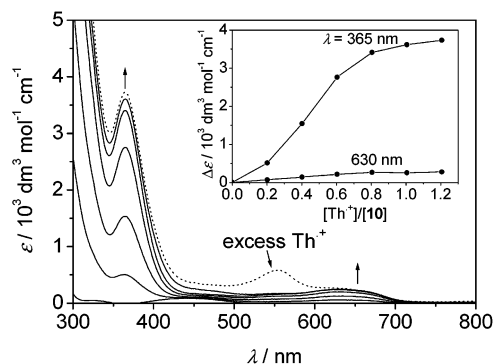


**Figure 6.** Spectral changes of ferrocenylpentanoic acid 4-methoxyphenyl ester **10** upon oxidation with thianthrenium pentachloroantimonate. (Inset) The absorption changes are plotted as the function of  $[\text{Th}^+]/[\mathbf{10}]$ .

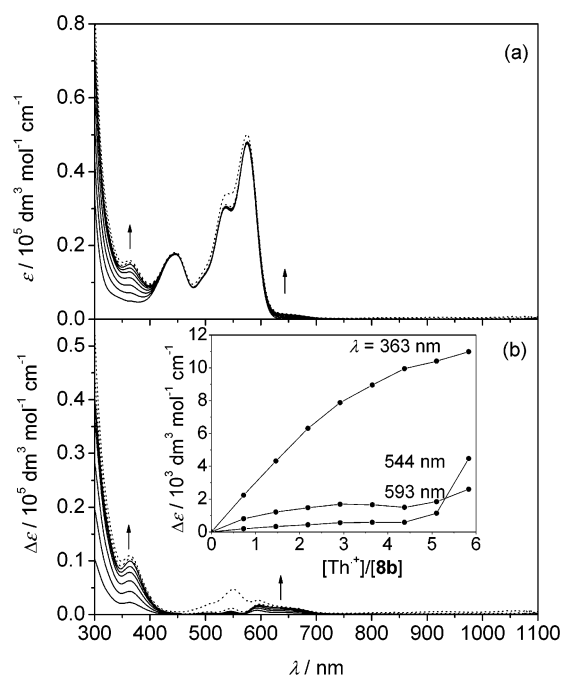


**Figure 7.** UV/vis spectra (a) and differential UV/vis spectra (b) of ferrocenyl-functionalized perylene bisimide **8b** upon oxidation with thianthrenium pentachloroantimonate; the dotted lines indicate that the amount of thianthrenium pentachloroantimonate is excess. (Inset) The absorption changes are plotted as the function of  $[\text{Th}^+]/[\mathbf{8b}]$ .

thianthrenium was employed. These results demonstrate that  $\text{Th}^+$  is properly suited for the oxidation of ferrocenyl derivatives and the redox titration can be conveniently followed by simple UV/vis spectroscopy.

Next, the redox titration of the ferrocenyl-substituted perylene bisimide **8b** with thianthrenium pentachloroantimonate was performed. From Figure 7, it can be seen that the addition of  $\text{Th}^+$  causes a substantial increase in absorption around 360 and 650 nm. To visualize the spectral changes upon addition of  $\text{Th}^+$ , the initial spectrum of **8b** was subtracted to obtain the differential UV/vis spectra (Figure 7b), which are shown to be similar to the corresponding spectra of model compound **10**. Because one molecule of **8b** contains four ferrocenyl units, after oxidation the molar extinction coefficients of **8b** at 365 and 630 nm are almost 4 times of those for compound **10**. In addition, the absorption of  $\text{Th}^+$  at 550 nm appeared once the  $[\text{Th}^+]/[\mathbf{8b}]$  ratio was over 4. These results clearly demonstrate that all four

- (26) (a) Han, D. S.; Shine, H. J. *J. Org. Chem.* **1996**, *61*, 3977–3982. (b) van Harre, J. A. E. H.; Havinga, E. E.; van Dongen, J. L. J.; Janssen, R. A. J.; Cornil, J.; Brédas, J.-L. *Chem.—Eur. J.* **1998**, *4*, 1509–1522. (c) Apperloo, J. J.; Langeveld-Voss, B. M. W.; Knol, J.; Hummelen, J. C.; Janssen, R. A. J. *Adv. Mater.* **2000**, *12*, 908–911.
- (27) Houmam, A.; Shukla, D.; Kraatz, H.-B.; Wayner, D. D. M. *J. Org. Chem.* **1999**, *64*, 3342–3345.
- (28) (a) Traverso, O.; Scandola, F. *Inorg. Chim. Acta* **1970**, *4*, 493–498. (b) Thander, A.; Mallik, B. *Proc. Indian Acad. Sci., Chem. Sci.* **2000**, *112*, 475–485.



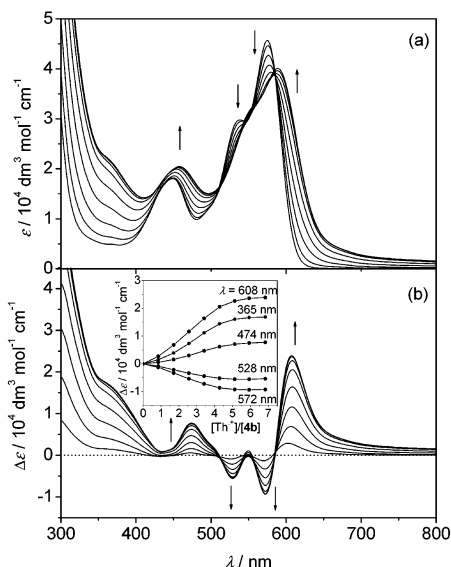


**Figure 8.** UV/vis spectra (a) and differential UV/vis spectra (b) of ditopic perylene ligand **4b** upon oxidation with thianthrenium pentachloroantimonate. (Inset) The absorption changes are plotted as the function of  $[\text{Th}^{+}]/[\mathbf{4b}]$ .

ferrocenyl substituents were transformed to ferroceniums by oxidation with  $\text{Th}^{+}$ .

Interestingly, ditopic perylene ligand **4b** exhibits more pronounced spectral changes upon oxidation by thianthrenium pentachloroantimonate. From Figure 8, it can be seen that the addition of  $\text{Th}^{+}$  causes a significant bathochromic shift of the absorption band of ligand **4b**. The differential UV/vis spectra (Figure 8b) show that pronounced changes occurred at around 608, 572, 528, 474, and 365 nm. The absorption changes at these wavelengths were plotted as a function of  $[\text{Th}^{+}]/[\mathbf{4b}]$ . This plot clearly shows that the curves, particularly at 365 nm (which is inherent for ferrocenium), reach a plateau when the ratio of  $[\text{Th}^{+}]/[\mathbf{4b}]$  is about 4. These results suggest that all four ferrocenyl units in perylene ligand **4b** were oxidized. Because of the large difference in the oxidation potentials of ferrocene and perylene functions, at the beginning of titration only the ferrocenyl moieties should be oxidized, though the perylene core has shown to be oxidizable by  $\text{Th}^{+}$  (see Figures S11 and S12 in the Supporting Information). However, the spectrum of compound **4b** changed drastically even with the addition of the first aliquot of  $\text{Th}^{+}$ , indicating that an interaction between the aza perylene lone pairs and thianthrenium pentachloroantimonate takes place. Indeed, a series of control experiments on redox titrations (see the Supporting Information, Figures S13 and S14) of 4,4'-bispyridine and *N,N'*-di(4-pyridyl)-1,6,7,12-tetra(4-*tert*-butylphenoxy)perylene-3,4:9,10-tetracarboxylic acid bisimide and its mixture with the model ferrocenyl derivative **10** revealed that the Lewis acidic  $\text{SbCl}_5$  generated from the counterion of the oxidant can interact with the pyridyl base to form adduct complexes.<sup>29</sup> Such complexation of the pyridine lone pairs of dipyridyl perylene ligand **4b** may lead to the spectral changes observed between 450 and 700 nm (Figure 8), which belong to the absorption bands of the perylene bisimide chromophore. A similar bathochromic shift of perylene

absorption bands has been observed upon protonation of pyridine units in structural analogues of **4b**.<sup>30</sup> Thus, thianthrenium pentachloroantimonate not only oxidizes effectively the ferrocenyl units in the ditopic perylene ligand **4b** but also undergoes complexation processes.

Very similar spectral changes, as in the case of ligand **4b**, were observed in the oxidation of the corresponding molecular square **9b** by thianthrenium pentachloroantimonate (see Figure S15 in the Supporting Information). Accordingly, the molecular square **9b** behaves like the free ligand **4b** upon interaction with thianthrenium pentachloroantimonate, suggesting that herein antimony pentachloride replaces  $\text{Pt}(\text{II})$  corners to coordinate more strongly to the pyridyl ligand and the square assembly gets decomposed.

The results of these redox titration studies confirm that ferrocene-substituted perylene bisimides may be chemically oxidized by thianthrenium pentachloroantimonate, and the redox process can be conveniently monitored by UV/vis spectroscopy. Complete oxidation of ferrocenyl moieties may be achieved in all ferrocene-functionalized perylene bisimides. In the case of ligands **4** and squares **9**, additional coordination interaction between the lone pairs of pyridyl and the counterion of oxidant takes place, while extended oxidation of ferrocenyl functions in the square causes its rupture. These results again demonstrate the lability of  $\text{Pt}(\text{II})$ -based molecular squares that easily decompose upon oxidative charging of the ferrocene units or coordinate to a more Lewis acidic metal.

## Conclusion

Through metallosupramolecular coordination strategy, perylene bispyridyl imides containing four ferrocenyl moieties could be organized to give molecular squares containing 20 redox active units. For the inner scaffold of four perylene bisimides, two reversible four-electron reductive processes that are little influenced by the supramolecular arrangement could be observed by cyclic voltammetry. In contrast, it has been found that the redox properties of the 16 peripheral ferrocenyl subunits are strongly affected by the sterical constraints imposed by the core square superstructure. In addition to electrochemical oxidation, also chemical oxidation of ferrocene-functionalized perylene bisimides could be realized by using thianthrenium pentachloroantimonate and the redox process could be conveniently monitored by spectrophotometry. The present study shows that metal-directed self-assembly of square structures can be used to organize redox active functional units in three-dimensional space.<sup>31</sup>

## Experimental Section

**Materials and Methods.** Solvents and reagents were purchased from Merck unless otherwise stated and purified and dried according to standard procedures.<sup>32</sup> 1,6,7,12-Tetra(4-butyloxyphenoxy)perylene-3,4:9,10-tetracarboxylic acid bisanhydride (**1**),<sup>18</sup> *N,N'*-di(2,6-diisopropylphenyl)-1,6,7,12-tetraphenoxyperylene-3,4:9,10-tetracarboxylic acid bisimide (**5**),<sup>20</sup> ferrocenylbutyric acid and ferrocenylvaleric acid,<sup>33</sup>  $[\text{Pt}(\text{dppp})][(\text{OTf})_2] \cdot 2\text{H}_2\text{O}$  (dppp = 1,3-bis(diphenylphosphino)propane; OTf = trifluoromethanesulfonate),<sup>21</sup> and thianthrenium pentachloro-

(29) Antimony pentachloride has been reported to complex with pyridine; for examples, see: (a) Holmes, R. R.; Gallagher, W. P.; Carter, Jr. R. P. *Inorg. Chem.* **1963**, *2*, 437–441. (b) Lim, Y. Y.; Drago, R. S. *Inorg. Chem.* **1972**, *11*, 202–204.

(30) Sautter, A. Ph.D. Thesis, University of Ulm, 2001.

(31) Grayson, S. M.; Fréchet, J. M. J. *Chem. Rev.* **2001**, *101*, 3819–3868.

(32) Perrin, D. D.; Armarego, W. L. F. *Purification of Laboratory Chemicals*, 2nd ed.; Pergamon Press: Oxford, 1980.

(33) (a) Rinehart, K. L.; Curby, R. J.; Sokol, P. E. *J. Am. Chem. Soc.* **1957**, *79*, 3420–3424. (b) Suzuki, I.; Chen, Q.; Ueno, A.; Osa, T. *Bull. Chem. Soc. Jpn.* **1993**, *66*, 1472–1481.

antimonate<sup>34</sup> were synthesized according to the literature procedure. Column chromatography was performed on silica gel (Merck Silica 60, particle size 0.04–0.63 mm). The solvents for spectroscopic studies were of spectroscopic grade and used as received. NMR spectra were recorded on a Bruker DRX 400 or AMX 500 spectrometer using TMS as internal standard. The <sup>31</sup>P{<sup>1</sup>H} NMR spectra were taken at 202 MHz, and chemical shifts are reported relative to external 85% aqueous H<sub>3</sub>PO<sub>4</sub> ( $\delta = 0$  ppm). MALDI-TOF spectra were recorded on a Bruker Franzen Reflex III spectrometer.

**Electrochemistry.** Cyclic voltammetry was performed with an EG&G PAR 273 potentiostat in a three-electrode single-compartment cell using dichloromethane as solvent (5 mL). Working electrode, platinum disk; counter electrode, platinum wire; reference electrode, Ag/AgCl. All potentials were internally referenced to the Fc/Fc<sup>+</sup> couple. The solutions were purged with argon gas prior to use. The supporting electrolyte was 0.1 M [Bu<sub>4</sub>N][PF<sub>6</sub>] (Fluka), which was recrystallized twice from ethanol/water and dried under high vacuum. The experimental setup for spectroelectrochemistry has been described by Salbeck.<sup>35</sup>

**Redox Titration.** UV/vis spectra were measured in a conventional quartz cell (light path 10 mm) on a Perkin–Elmer Lambda 40P spectrophotometer at room temperature (ca. 20 °C). For redox-titration experiments, 2 mL of the sample solution in CH<sub>2</sub>Cl<sub>2</sub> (the concentration of ferrocenyl moieties is about 0.1 mM) was placed in the cuvette and the initial spectrum was recorded. Aliquots of a freshly prepared thianthrenium pentachloroantimonate solution in CH<sub>2</sub>Cl<sub>2</sub> (0.2 mM) were subsequently added to the sample solution in the cuvette. After each addition, a UV/vis spectrum was recorded. The spectra obtained were then normalized based on the concentration of perylene bisimide samples according to the Beer–Lambert law ( $\epsilon = A/c \cdot l$ ). To visualize the minor spectral changes, differential UV/vis spectra were also presented in the results by simply subtracting the initial spectrum.

**Molecular Modeling.** To get insight into the steric demand and a possible arrangement of the appendant ferrocenyl substituents within molecular square **9**, molecular modeling and molecular dynamics simulation (MD-MM2) were carried out by using CAChe 5.0 (Oxford Molecular 2000). The augmented force field was used with parametrization of transition metals. Molecular dynamics simulations (MD-MM2, in vacuo at a temperature of  $T = 300$  K) implemented in the CAChe 5.0 program package were applied.

***N,N'*-Di(4-pyridyl)-1,6,7,12-tetra(4-butyloxyphenoxy)perylene-3,4:9,10-tetracarboxylic Acid Bisimide (2).** A mixture of perylene-3,4:9,10-tetracarboxylic acid bisanhydride **1** (1.05 g, 1.0 mmol), 4-aminopyridine (0.33 g, 3.5 mmol), and zinc acetate (0.1 g, 0.55 mmol) in quinoline (30 mL) was stirred under argon at 180 °C for 16 h. After the solution was chilled, 2 M hydrochloric acid (150 mL) was added to precipitate the product, which was collected by suction filtration and washed thoroughly with a large amount of water and dried in a vacuum. The crude product was purified by column chromatography (SiO<sub>2</sub>) with CH<sub>2</sub>Cl<sub>2</sub>/CH<sub>3</sub>OH (98:2) as eluent. After evaporation of the solvent, the bisimide **2** was obtained as a dark purple powder. Yield 0.65 g (54%); mp > 300 °C. <sup>1</sup>H NMR (CDCl<sub>3</sub>):  $\delta$  8.74 (d, <sup>3</sup>*J* = 6.1 Hz, 4H, H <sub>$\alpha$ -py</sub>), 8.07 (s, 4H, H<sub>per</sub>), 7.21 (d, <sup>3</sup>*J* = 6.1 Hz, 4H, H <sub>$\beta$ -py</sub>), 6.87 (d, <sup>3</sup>*J* = 9.1 Hz, 8H, H<sub>ar</sub>), 6.80 (d, <sup>3</sup>*J* = 9.1 Hz, 8H, H<sub>ar</sub>), 3.91 (t, 8H, –OCH<sub>2</sub>–), 1.76 (m, 8H), 1.50 (m, 8H), 0.99 (t, 12H, –CH<sub>3</sub>). MS (MALDI-TOF, dithranol): *m/z* 1200.3 [M]<sup>+</sup> (calcd for C<sub>74</sub>H<sub>64</sub>N<sub>4</sub>O<sub>12</sub> 1200.5). Anal. Calcd for C<sub>74</sub>H<sub>64</sub>N<sub>4</sub>O<sub>12</sub>: C, 73.99; H, 5.37; N, 4.66. Found: C, 73.70; H, 5.27; N, 4.64.

***N,N'*-Di(4-pyridyl)-1,6,7,12-tetra(4-hydroxyphenoxy)perylene-3,4:9,10-tetracarboxylic Acid Bisimide (3).** BBr<sub>3</sub> (0.5 mL, 5.3 mmol) in dry CH<sub>2</sub>Cl<sub>2</sub> (20 mL) was added dropwise to a stirred solution of bis-

(pyridyl)perylene **2** (385 mg, 0.32 mmol) in dry CH<sub>2</sub>Cl<sub>2</sub> (250 mL) at room temperature (ca. 20 °C). After the solution was stirred for an additional 2 h at room temperature, the solvent was removed by distillation and the residue was carefully hydrolyzed with ice-cold water (40 mL). Then methanol (20 mL) was added, and the suspension was boiled for 1 min. The precipitate was collected by centrifugation, washed with water (10 mL  $\times$  3), and dried in vacuo at 90 °C. Yield 320 mg (92%); mp > 300 °C. <sup>1</sup>H NMR (DMSO-*d*<sub>6</sub>):  $\delta$  9.47 (br s, 4H, H<sub>OH</sub>), 8.78 (d, <sup>3</sup>*J* = 6.2 Hz, 4H, H <sub>$\alpha$ -py</sub>), 7.82 (s, 4H, H<sub>per</sub>), 7.54 (d, <sup>3</sup>*J* = 6.2 Hz, 4H, H <sub>$\beta$ -py</sub>), 6.84 (d, <sup>3</sup>*J* = 9.0 Hz, 8H, H<sub>ar</sub>), 6.73 (d, <sup>3</sup>*J* = 9.0 Hz, 8H, H<sub>ar</sub>). MS (MALDI-TOF, dithranol): *m/z* 976.2 [M]<sup>+</sup> (calcd for C<sub>58</sub>H<sub>32</sub>N<sub>4</sub>O<sub>12</sub> 976.2). Anal. Calcd for C<sub>58</sub>H<sub>32</sub>N<sub>4</sub>O<sub>12</sub>·6H<sub>2</sub>O: C, 64.21; H, 4.09; N, 5.16. Found: C, 64.49; H, 4.07; N, 4.84.

***N,N'*-Di(4-pyridyl)-1,6,7,12-tetra(4-(4-ferrocenyl)butanoyloxyphenoxy)perylene-3,4:9,10-tetracarboxylic Acid Bisimide (4a).** Perylene bisimide **3** (88.3 mg, 0.081 mmol), ferrocenylbutyric acid (176 mg, 0.65 mmol), DPTS (235 mg, 0.80 mmol), and DCC (206 mg, 1.0 mmol) were dissolved in a mixture of DMF (4 mL) and CH<sub>2</sub>Cl<sub>2</sub> (10 mL) and stirred at room temperature (ca. 20 °C) for 3 h. Subsequently, another portion of DCC (206 mg) and a small amount of molecular sieve (4 Å) were added, and the mixture was stirred at room temperature for 3 d. Dichloromethane (40 mL) was added to the reaction mixture, and the undissolved material was removed by filtration. The filtrate was concentrated to ca. 4 mL, and 40 mL of methanol was added to precipitate the crude product, which was collected by centrifugation and washed with methanol. After the sample was dried in air, it was purified by column chromatography (SiO<sub>2</sub>) with CH<sub>2</sub>Cl<sub>2</sub>/EtOH (95:5) as eluent. Yield 31 mg (19%); mp > 300 °C. <sup>1</sup>H NMR (CDCl<sub>3</sub>):  $\delta$  8.79 (d, <sup>3</sup>*J* = 5.9 Hz, 4H, H <sub>$\alpha$ -py</sub>), 8.25 (s, 4H, H<sub>per</sub>), 7.25 (d, <sup>3</sup>*J* = 5.9 Hz, 4H, H <sub>$\beta$ -py</sub>, overlapped with CHCl<sub>3</sub> signal), 7.03 (d, <sup>3</sup>*J* = 9.1 Hz, 8H, H<sub>ar</sub>), 6.91 (d, <sup>3</sup>*J* = 9.1 Hz, 8H, H<sub>ar</sub>), 4.12 (s, 20H, H<sub>ferro</sub>), 4.08 (m, 16H, H<sub>ferro</sub>), 2.56 (t, 8H, –CH<sub>2</sub>–), 2.46 (t, 8H, –CH<sub>2</sub>–), 1.94 (m, 8H, –CH<sub>2</sub>–). UV/vis (CH<sub>2</sub>Cl<sub>2</sub>):  $\lambda_{\max}$  ( $\epsilon$ ) = 574 (44 300), 536 (28 700), 448 (17 700), 266 nm (57 300 dm<sup>3</sup> mol<sup>–1</sup> cm<sup>–1</sup>). MS (MALDI-TOF, dithranol): *m/z* 1992.6 [M]<sup>+</sup> (calcd for C<sub>114</sub>H<sub>88</sub>Fe<sub>4</sub>N<sub>4</sub>O<sub>16</sub> 1992.4). Anal. Calcd for C<sub>114</sub>H<sub>88</sub>Fe<sub>4</sub>N<sub>4</sub>O<sub>16</sub>: C, 68.69; H, 4.45; N, 2.81. Found: C, 68.67; H, 4.58; N, 2.69.

***N,N'*-Di(4-pyridyl)-1,6,7,12-tetra(4-(5-ferrocenyl)pentanoyloxyphenoxy)perylene-3,4:9,10-tetracarboxylic Acid Bisimide (4b).** Compound **4b** was prepared by the esterification of *N,N'*-di(4-pyridyl)-1,6,7,12-tetra(4-hydroxyphenoxy)perylene-3,4:9,10-tetracarboxylic acid bisimide (**3**) (109 mg, 0.1 mmol) with ferrocenylvaleric acid (286 mg, 1.0 mmol) according to the above procedure. Yield 54 mg (26%); mp > 300 °C. <sup>1</sup>H NMR (CDCl<sub>3</sub>):  $\delta$  8.79 (d, <sup>3</sup>*J* = 6.1 Hz, 4H, H <sub>$\alpha$ -py</sub>), 8.24 (s, 4H, H<sub>per</sub>), 7.25 (d, <sup>3</sup>*J* = 6.1 Hz, 4H, H <sub>$\beta$ -py</sub>, overlapped with CHCl<sub>3</sub> signal), 7.02 (d, <sup>3</sup>*J* = 9.1 Hz, 8H, H<sub>ar</sub>), 6.91 (d, <sup>3</sup>*J* = 9.1 Hz, 8H, H<sub>ar</sub>), 4.10 (s, 20H, H<sub>ferro</sub>), 4.07 (m, 16H, H<sub>ferro</sub>), 2.55 (t, 8H, –CH<sub>2</sub>–), 2.40 (t, 8H, –CH<sub>2</sub>–), 1.78 (m, 8H, –CH<sub>2</sub>–), 1.62 (m, 8H, –CH<sub>2</sub>–); UV/vis (CH<sub>2</sub>Cl<sub>2</sub>):  $\lambda_{\max}$  ( $\epsilon$ ) = 574 (44 800), 537 (29 200), 448 (17 700), 266 nm (57 500 dm<sup>3</sup> mol<sup>–1</sup> cm<sup>–1</sup>). MS (MALDI-TOF, dithranol): *m/z* 2048.4 [M]<sup>+</sup> (calcd for C<sub>118</sub>H<sub>96</sub>Fe<sub>4</sub>N<sub>4</sub>O<sub>16</sub> 2048.4). Anal. Calcd for C<sub>118</sub>H<sub>96</sub>Fe<sub>4</sub>N<sub>4</sub>O<sub>16</sub>: C, 69.15; H, 4.72; N, 2.73. Found: C, 69.27; H, 4.80; N, 2.66.

***N,N'*-Di(2,6-diisopropylphenyl)-1,6,7,12-tetra(4-butyloxyphenoxy)perylene-3,4:9,10-tetracarboxylic Acid Bisimide (6).** Tetrachloropyrene bisimide **5** (2.55 g, 3.0 mmol), 4-butyloxyphenol (2.50 g, 15.0 mmol), and K<sub>2</sub>CO<sub>3</sub> (2.10 g, 15.0 mmol) were suspended in *N*-methyl pyrrolidone (80 mL) and stirred under argon at 160 °C for 6 h. After the solution was cooled to room temperature, dilute HCl (2 M, 100 mL) was added to precipitate the crude product, which was collected by suction filtration and washed successively with water and methanol. After the sample was dried in air, it was purified by column chromatography (SiO<sub>2</sub>) with dichloromethane as eluent. Yield 1.37 g (33%); mp > 300 °C. <sup>1</sup>H NMR (CDCl<sub>3</sub>):  $\delta$  8.17 (s, 4H, H<sub>per</sub>), 7.42 (t, 2H, H<sub>ar</sub>), 7.26 (d, <sup>3</sup>*J* = 7.7 Hz, 4H, H<sub>ar</sub>), 6.93 (d, <sup>3</sup>*J* = 9.1 Hz, 8H, H<sub>ar</sub>), 6.81 (d, <sup>3</sup>*J* = 9.1 Hz, 8H, H<sub>ar</sub>), 3.92 (t, 8H, –OCH<sub>2</sub>–), 2.69

(34) (a) Lucken, E. A. C. *J. Chem. Soc.* **1962**, 4963–4965. (b) Kinoshits, M. *Bull. Chem. Soc. Jpn.* **1962**, 35, 1137–1140. (c) Balch, A. L.; Cornman, C. R.; Latos-Grazyński, L.; Olmstead, M. M. *J. Am. Chem. Soc.* **1990**, 112, 7552–7558.

(35) Salbeck, J. *J. Electroanal. Chem.* **1992**, 340, 169–195.

(m, 4H,  $-\text{CH}<$ ), 1.75 (m, 8H,  $-\text{CH}_2-$ ), 1.49 (m, 8H,  $-\text{CH}_2-$ ), 1.11 (d,  $^3J = 6.8$  Hz, 24H,  $-\text{CH}_3$ ), 0.98 (t, 12H,  $-\text{CH}_3$ ); UV/vis ( $\text{CH}_2\text{Cl}_2$ ):  $\lambda_{\text{max}}$  ( $\epsilon$ ) = 591 (52 700), 548 (30 400), 457 (16 100), 286 (51 200), 268 nm ( $49\ 300\ \text{dm}^3\ \text{mol}^{-1}\ \text{cm}^{-1}$ ). MS (MALDI-TOF, dithranol):  $m/z$  1367.6  $[\text{M} + \text{H}]^+$  (calcd for  $\text{C}_{88}\text{H}_{90}\text{N}_2\text{O}_{12}$  1367.6). Anal. Calcd for  $\text{C}_{88}\text{H}_{90}\text{N}_2\text{O}_{12}$ : C, 77.28; H, 6.63; N, 2.05. Found: C, 76.90; H, 6.79; N, 1.90.

***N,N'*-Di(2,6-diisopropylphenyl)-1,6,7,12-tetra(4-hydroxyphenoxy)perylene-3,4:9,10-tetracarboxylic Acid Bisimide (7).** Compound **7** was prepared by the reaction of perylene bisimide **6** (0.55 g, 0.40 mmol) with  $\text{BBR}_3$  (1 M, 20 mL) in dry  $\text{CH}_2\text{Cl}_2$  and worked up in the same way as described for **3**. Yield 0.37 g (81%); mp > 300 °C.  $^1\text{H}$  NMR ( $\text{DMSO-}d_6$ ):  $\delta$  9.49 (s, 4H, OH), 7.88 (s, 4H,  $\text{H}_{\text{per}}$ ), 7.41 (t, 2H,  $\text{H}_{\text{ar}}$ ), 7.29 (d, 4H,  $\text{H}_{\text{ar}}$ ), 6.93 (d,  $^3J = 8.8$  Hz, 8H,  $\text{H}_{\text{ar}}$ ), 6.78 (d,  $^3J = 8.8$  Hz,  $\text{H}_{\text{ar}}$ ), 2.66 (m, 4H,  $-\text{CH}<$ ), 1.01 (d, 24H,  $-\text{CH}_3$ ). UV/vis ( $\text{CH}_3\text{OH}$ ):  $\lambda_{\text{max}}$  ( $\epsilon$ ) = 596 (49 800), 555 (29 500), 459 (14 700), 283 (47 400), 268 nm ( $48\ 600\ \text{dm}^3\ \text{mol}^{-1}\ \text{cm}^{-1}$ ). MS (MALDI-TOF, dithranol):  $m/z$  1143.5  $[\text{M} + \text{H}]^+$  (calcd for  $\text{C}_{72}\text{H}_{58}\text{N}_2\text{O}_{12}$  1143.4). Anal. Calcd for  $\text{C}_{72}\text{H}_{58}\text{N}_2\text{O}_{12}\cdot\text{H}_2\text{O}$ : C, 74.47; H, 5.21; N, 2.41. Found: C, 74.40; H, 5.26; N, 2.28.

***N,N'*-Di(2,6-diisopropylphenyl)-1,6,7,12-tetra(4-(4-ferrocenyl)butanoyloxy-phenoxy)perylene-3,4:9,10-tetracarboxylic Acid Bisimide (8a).** Compound **8a** was synthesized by the esterification of *N,N'*-di(2,6-diisopropylphenyl)-1,6,7,12-tetra(4-hydroxyphenoxy)perylene-3,4:9,10-tetracarboxylic acid bisimide (**7**) (116 mg, 0.1 mmol) with ferrocenylbutyric acid (272 mg, 1.0 mmol) in the presence of DCC and DPTS according to the procedure described for **4a**. The product was purified by column chromatography ( $\text{SiO}_2$ ) with chloroform as eluent. Yield 32 mg (15%); mp 170–171 °C.  $^1\text{H}$  NMR ( $\text{CDCl}_3$ ):  $\delta$  8.28 (s, 4H,  $\text{H}_{\text{per}}$ ), 7.44 (t, 2H,  $\text{H}_{\text{ar}}$ ), 7.28 (d, 4H,  $\text{H}_{\text{ar}}$ ), 7.04 (d,  $^3J = 9.1$  Hz, 8H,  $\text{H}_{\text{ar}}$ ), 6.94 (d,  $^3J = 9.1$  Hz, 8H,  $\text{H}_{\text{ar}}$ ), 4.11 (s, 20H,  $\text{H}_{\text{ferro}}$ ), 4.08 (m, 16H,  $\text{H}_{\text{ferro}}$ ), 2.70 (m, 4H,  $-\text{CH}<$ ), 2.55 (t, 8H,  $-\text{CH}_2\text{CO}-$ ), 2.45 (t, 8H,  $\text{Fc}-\text{CH}_2-$ ), 1.94 (m, 8H,  $-\text{CH}_2-$ ), 1.13 (d, 24H,  $-\text{CH}_3$ ). UV/vis ( $\text{CH}_2\text{Cl}_2$ ):  $\lambda_{\text{max}}$  ( $\epsilon$ ) = 573 (46 500), 535 (29 500), 444 (17 300), 282 (52 600), 264 nm ( $56\ 700\ \text{dm}^3\ \text{mol}^{-1}\ \text{cm}^{-1}$ ). MS (MALDI-TOF, dithranol):  $m/z$  2158.6  $[\text{M}]^+$  (calcd for  $\text{C}_{128}\text{H}_{114}\text{Fe}_4\text{N}_2\text{O}_{16}$  2158.6). Anal. Calcd for  $\text{C}_{128}\text{H}_{114}\text{Fe}_4\text{N}_2\text{O}_{16}$ : C, 71.19; H, 5.32; N, 1.30. Found: C, 71.30; H, 5.44; N, 1.23.

***N,N'*-Di(2,6-diisopropylphenyl)-1,6,7,12-tetra(4-(5-ferrocenyl)pentanoyloxy-phenoxy)perylene-3,4:9,10-tetracarboxylic Acid Bisimide (8b).** Compound **8b** was synthesized by the esterification of *N,N'*-di(2,6-diisopropylphenyl)-1,6,7,12-tetra(4-hydroxyphenoxy)perylene-3,4:9,10-tetracarboxylic acid bisimide (**7**) (116 mg, 0.1 mmol) and ferrocenylvaleric acid (286 mg, 1.0 mmol) in the presence of DCC and DPTS according to the procedure described for **4a**. Yield 63 mg (28%); mp 175–176 °C.  $^1\text{H}$  NMR ( $\text{CDCl}_3$ ):  $\delta$  8.28 (s, 4H,  $\text{H}_{\text{per}}$ ), 7.44 (t, 2H,  $\text{H}_{\text{ar}}$ ), 7.28 (d, 4H,  $\text{H}_{\text{ar}}$ ), 7.03 (d,  $^3J = 9.2$  Hz, 8H,  $\text{H}_{\text{ar}}$ ), 6.93 (d,  $^3J = 9.2$  Hz, 8H,  $\text{H}_{\text{ar}}$ ), 4.09 (s, 20H,  $\text{H}_{\text{ferro}}$ ), 4.06 (m, 16H,  $\text{H}_{\text{ferro}}$ ), 2.70 (m, 4H,  $-\text{CH}<$ ), 2.55 (t, 8H,  $-\text{CH}_2\text{CO}-$ ), 2.42 (t, 8H,  $\text{Fc}-\text{CH}_2-$ ), 1.78 (m, 8H,  $-\text{CH}_2-$ ), 1.62 (m, 8H,  $-\text{CH}_2-$ ), 1.13 (d, 24H,  $-\text{CH}_3$ ). UV/vis ( $\text{CH}_2\text{Cl}_2$ ):  $\lambda_{\text{max}}$  ( $\epsilon$ ) = 573 (47 600), 535 (30 200), 444 (17 500), 282 (53 300), 264 nm ( $57\ 400\ \text{dm}^3\ \text{mol}^{-1}\ \text{cm}^{-1}$ ). MS (MALDI-TOF, dithranol):  $m/z$  2214.2  $[\text{M}]^+$  (calcd for  $\text{C}_{132}\text{H}_{122}\text{Fe}_4\text{N}_2\text{O}_{16}$  2214.6). Anal. Calcd for  $\text{C}_{132}\text{H}_{122}\text{Fe}_4\text{N}_2\text{O}_{16}$ : C, 71.55; H, 5.55; N, 1.26. Found: C, 71.44; H, 5.62; N, 1.27.

**Ferrocene-Containing Perylene Bisimide Platinum Square 9a.** A 1:1 stoichiometric mixture of *N,N'*-di(4-pyridyl)-1,6,7,12-tetra(4-(4-ferrocenyl)butanoyloxy-phenoxy)perylene-3,4:9,10-tetracarboxylic acid bisimide (**4a**) (19.93 mg, 10.0  $\mu\text{mol}$ ) and  $[\text{Pt}(\text{dppp})][(\text{OTf})_2]\cdot 2\text{H}_2\text{O}$  (9.42 mg, 10.0  $\mu\text{mol}$ ) in  $\text{CH}_2\text{Cl}_2$  (5 mL) was stirred at room temperature (ca. 20 °C) for 24 h. After filtration, the solution was concentrated to ca. 1

mL, and diethyl ether (10 mL) was added to precipitate the product, which was collected by centrifugation and washed with ether (10 mL  $\times$  2). After the product was dried in a vacuum, a dark red powder was obtained. Yield 20 mg (68%); mp > 300 °C.  $^1\text{H}$  NMR ( $\text{CDCl}_3$ ):  $\delta$  9.14 (br s, 16H,  $\text{H}_{\alpha\text{-py}}$ ), 8.15 (s, 16H,  $\text{H}_{\text{per}}$ ), 7.67 (br s, 32H,  $\text{H}_{\text{dppp}}$ ), 7.40 (br m, 48H,  $\text{H}_{\text{dppp}}$ ), 7.11 (br d, 16H,  $\text{H}_{\beta\text{-py}}$ ), 6.98 (d,  $^3J = 8.9$  Hz, 32H,  $\text{H}_{\text{ar}}$ ), 6.86 (d,  $^3J = 8.9$  Hz, 32H,  $\text{H}_{\text{ar}}$ ), 4.25 (br s, 144H,  $\text{H}_{\text{ferro}}$ ), 3.29 (br s, 16H,  $\text{H}_{\text{dppp}}$ ), 2.49 (m, 32H,  $-\text{CH}_2-$ ), 2.21 (br s, 40H,  $\text{H}_{\text{dppp}}$  +  $-\text{CH}_2-$ ), 1.79 (br s, 32H,  $-\text{CH}_2-$ ).  $^{31}\text{P}\{^1\text{H}\}$  NMR ( $\text{CDCl}_3$ ):  $\delta$  -15.29 (s,  $^1J_{\text{Pt-P}} = 3084$  Hz). UV/vis ( $\text{CH}_2\text{Cl}_2$ ):  $\lambda_{\text{max}}$  ( $\epsilon$ ) = 579 (186 100), 543 (126 700), 452 nm ( $67\ 300\ \text{dm}^3\ \text{mol}^{-1}\ \text{cm}^{-1}$ ). Anal. Calcd for  $\text{C}_{572}\text{H}_{456}\text{F}_{24}\text{Fe}_{16}\text{N}_{16}\text{O}_{16}\text{P}_4\text{S}_8\cdot 8\text{H}_2\text{O}$ : C, 58.52; H, 4.05; N, 1.91; S, 2.18. Found: C, 58.41; H, 4.03; N, 1.89; S, 2.30.

**Ferrocene-Containing Perylene Bisimide Platinum Square 9b.** *N,N'*-Di(4-pyridyl)-1,6,7,12-tetra(4-(5-ferrocenyl)pentanoyloxy-phenoxy)perylene-3,4:9,10-tetracarboxylic acid bisimide (**4b**) (20.49 mg, 10.0  $\mu\text{mol}$ ) and  $[\text{Pt}(\text{dppp})][(\text{OTf})_2]\cdot 2\text{H}_2\text{O}$  (9.42 mg, 10.0  $\mu\text{mol}$ ) were reacted and worked up according to the procedure described for **9a**. Yield 23 mg (77%); mp > 300 °C.  $^1\text{H}$  NMR ( $\text{CDCl}_3$ ):  $\delta$  9.14 (br s, 16H,  $\text{H}_{\alpha\text{-py}}$ ), 8.17 (s, 16H,  $\text{H}_{\text{per}}$ ), 7.66 (br s, 32H,  $\text{H}_{\text{dppp}}$ ), 7.40–7.30 (m, 48H,  $\text{H}_{\text{dppp}}$ ), 7.12 (d, 16H,  $\text{H}_{\beta\text{-py}}$ ), 6.97 (d,  $^3J = 8.9$  Hz, 32H,  $\text{H}_{\text{ar}}$ ), 6.86 (d,  $^3J = 8.9$  Hz, 32H,  $\text{H}_{\text{ar}}$ ), 4.27 (br s, 144H,  $\text{H}_{\text{ferro}}$ ), 3.29 (br s, 16H,  $\text{H}_{\text{dppp}}$ ), 2.46 (t, 32H,  $-\text{CH}_2-$ ), 2.15 (br s, 40H,  $\text{H}_{\text{dppp}}$  +  $-\text{CH}_2-$ ), 1.70 (m, 32H,  $-\text{CH}_2-$ ), 1.45 (br s, 32H,  $-\text{CH}_2-$ );  $^{31}\text{P}\{^1\text{H}\}$  NMR ( $\text{CDCl}_3$ ):  $\delta$  -15.33 (s,  $^1J_{\text{Pt-P}} = 3081$  Hz). UV/vis ( $\text{CH}_2\text{Cl}_2$ ):  $\lambda_{\text{max}}$  ( $\epsilon$ ) = 579 (191 200), 543 (130 500), 452 nm ( $69\ 200\ \text{dm}^3\ \text{mol}^{-1}\ \text{cm}^{-1}$ ). Anal. Calcd for  $\text{C}_{588}\text{H}_{488}\text{F}_{24}\text{Fe}_{16}\text{N}_{16}\text{O}_{16}\text{P}_4\text{S}_8\cdot 8\text{H}_2\text{O}$ : C, 59.03; H, 4.25; N, 1.87; S, 2.14. Found: C, 59.22; H, 4.22; N, 1.87; S, 2.26.

**5-Ferrocenylpentanoic Acid 4-Methoxyphenyl Ester (10).** A mixture of ferrocenylvaleric acid (572 mg, 2.0 mmol), 4-methoxyphenol (248 mg, 2.0 mmol), DCC (500 mg, 2.4 mmol), and DMAP (100 mg, 0.8 mmol) was dissolved in dry  $\text{CH}_2\text{Cl}_2$  (50 mL) and stirred at room temperature (ca. 20 °C) for 3 d. After filtration, the filtrate was concentrated, and the residue was purified by column chromatography ( $\text{SiO}_2$ ) with  $\text{CH}_2\text{Cl}_2$  as eluent. The desired eluting band was collected, and the solvent was evaporated to give a yellow oil, which became a solid after drying in a vacuum. Yield 520 mg (66%); mp 85–86 °C.  $^1\text{H}$  NMR ( $\text{CDCl}_3$ ):  $\delta$  6.98 (d,  $^3J = 9.1$  Hz, 2H,  $\text{H}_{\text{ar}}$ ), 6.87 (d,  $^3J = 9.1$  Hz, 2H,  $\text{H}_{\text{ar}}$ ), 4.09 (s, 5H,  $\text{H}_{\text{ferro}}$ ), 4.07 (m, 2H,  $\text{H}_{\text{ferro}}$ ), 4.04 (m, 2H,  $\text{H}_{\text{ferro}}$ ), 3.79 (s, 3H,  $-\text{OCH}_3$ ), 2.55 (t, 2H,  $-\text{CH}_2-$ ), 2.39 (t, 2H,  $-\text{CH}_2-$ ), 1.78 (m, 2H,  $-\text{CH}_2-$ ), 1.62 (m, 2H,  $-\text{CH}_2-$ ).  $^{13}\text{C}$  NMR ( $\text{CDCl}_3$ ):  $\delta$  172.49, 157.20, 144.25, 122.29, 114.45, 88.73, 68.49, 68.06, 67.15, 55.59, 34.20, 30.57, 29.29, 24.87. MS (EI, 70 eV):  $m/z$  392.1  $[\text{M}]^+$  (calcd for  $\text{C}_{22}\text{H}_{24}\text{FeO}_3$  392.1). Anal. Calcd for  $\text{C}_{22}\text{H}_{24}\text{FeO}_3$ : C, 67.36; H, 6.17. Found: C, 67.10; H, 6.32.

**Acknowledgment.** We thank the Alexander von Humboldt Foundation (fellowship for C.C.Y.) and the Fonds der Chemischen Industrie for financial support and BASF AG and Degussa-Hüls AG for the donation of chemicals. We are indebted to Dr. Günther Götz and Prof. Peter Bäuerle (Ulm) for their support in the electrochemical measurements and helpful discussions.

**Supporting Information Available:** NMR ( $^1\text{H}$  and  $^{31}\text{P}$ ) and UV spectra for molecular squares **9a** and **9b** and cyclic voltammograms and UV/vis spectra of redox titrations. This material is available free of charge via the Internet at <http://pubs.acs.org>.

JA029648X